

POLYNOMIAL-PHASE SIGNAL DIRECTION-FINDING AND SOURCE-TRACKING WITH A SINGLE ACOUSTIC VECTOR SENSOR

Xin Yuan, Jiaji Huang and Robert Calderbank

Department of Electrical and Computer Engineering, Duke University, Durham, NC, 27708, USA

ABSTRACT

This paper introduces a new ESPRIT-based algorithm to estimate the direction-of-arrival of an arbitrary degree polynomial-phase signal with a single acoustic vector-sensor. The proposed time-invariant ESPRIT algorithm is based on a matrix-pencil pair derived from the time-delayed data-sets collected by a single acoustic vector-sensor. This approach requires neither a prior knowledge of the polynomial-phase signal's coefficients nor a prior knowledge of the polynomial-phase signal's frequency-spectrum. Furthermore, a pre-processing technique is proposed to incorporate the single-forgetting-factor algorithm and multiple-forgetting-factor adaptive tracking algorithm to track a polynomial-phase signal using one acoustic vector sensor. Simulation results verify the efficacy of the proposed direction finding and source tracking algorithms.

Index Terms— Acoustic signal processing, direction of arrival estimation, eigenvalues and eigenfunctions, polynomial approximation, sonar.

1. INTRODUCTION

Direction finding with acoustic vector sensors has attracted much attention in recent years [1–14] since the acoustic vector sensor outperforms the conventional pressure sensor [1, 2, 8]. An acoustic vector sensor comprises three orthogonal velocity sensors, and a pressure sensor, which are collocated at a point geometry in space. The acoustic vector sensor can thus measure both pressure and particle velocity of the acoustic field at a point in space; whereas a traditional pressure sensor can only extract the pressure information. The response of an acoustic vector sensor to a far-field unity power incident acoustic wave can be characterized by [1]:

$$\mathbf{a} \stackrel{\text{def}}{=} \begin{bmatrix} \mathbf{u}_x(\alpha, \beta) \\ \mathbf{u}_y(\alpha, \beta) \\ \mathbf{u}_z(\alpha) \\ 1 \end{bmatrix} \stackrel{\text{def}}{=} \begin{bmatrix} \sin \alpha \cos \beta \\ \sin \alpha \sin \beta \\ \cos \alpha \\ 1 \end{bmatrix}, \quad (1)$$

where $\alpha \in [0, \pi]$, $\beta \in [0, 2\pi)$ are the elevation-angle and azimuth-angle of the source, and $\mathbf{u}_x, \mathbf{u}_y, \mathbf{u}_z$ symbolize the three Cartesian components of \mathbf{u} along each axis in the Cartesian coordinate system, respectively. Many advantages are offered by the acoustic vector sensor [9]: a) The array-manifold

is independent of the source's frequency spectrum. b) The array-manifold is less sensitive to the distance of the source. However, overlooked in the literature is how to estimate the direction-of-arrival of a polynomial-phase signal with an arbitrary degree.

Polynomial-phase signal (PPS) is a model used in a variety of applications. For example: radar, sonar, and communication systems use continuous-phase modulation where the amplitude is constant and the phase is a continuous function of time [15]. This function on a closed interval can be uniformly approximated by polynomials from the Weierstrass theorem [16]. The phase of the signal above can then be modeled as a finite-order polynomial within a finite-duration time-interval. A unity power polynomial-phase signal can be modeled in continuous time as:

$$s(t) = \exp \{j (b_0 + b_1 t + b_2 t^2 + \cdots + b_q t^q)\}, \quad (2)$$

where b_1, \dots, b_q are the polynomial coefficients associated with the corresponding orders, q is the degree of the polynomial-phase signal, and the initial phase is b_0 . When $q = 2$, the polynomial-phase signal is known as an LFM (linear frequency modulated) signal [17]. The polynomial-phase signal has received considerable attention in the literature [15, 18–23].

2. DIRECTION FINDING

Consider a polynomial-phase signal impinging upon an acoustic vector sensor. The collected 4×1 data vector at time t equals:

$$\mathbf{z}(t) = \mathbf{a}s(t) + \mathbf{n}(t), \quad (3)$$

where $\mathbf{n}(t)$ symbolizes the additive noise at the acoustic vector sensor, $s(t)$ is the polynomial-phase signal as in (2), and \mathbf{a} is the steering vector of the signal as in (1). In this work, $\mathbf{n}(t)$ is modeled as zero mean, complex Gaussian distributed, and with a covariance of a 4×4 diagonal matrix $\mathbf{K}_0 = \text{diag}[\sigma^2, \sigma^2, \sigma^2, \sigma^2]$, where σ^2 denotes the variance of noise collected by each constituent antenna. (This proposed algorithm can also be used in the three-component acoustic vector sensor as discussed in [6]) From (3):

$$\mathbf{z}(t) = \mathbf{a}s(t) + \mathbf{n}(t) = [\mathbf{u}_x, \mathbf{u}_y, \mathbf{u}_z, 1]^T s(t) + \mathbf{n}(t), \quad (4)$$

where T denotes the transposition. In order to simplify the exposition, we consider the *noiseless* case in the following derivation. Consider a q -order polynomial-phase signal, and

let $\mathbf{z}_{(q)}(t)$ be the measured data of the acoustic vector sensor for this signal. In the noiseless case:

$$\mathbf{z}_{(q)}(t) = [\mathbf{u}_x, \mathbf{u}_y, \mathbf{u}_z, 1]^T s(t). \quad (5)$$

$\mathbf{z}_{(q)}(t)$ is a 4×1 vector, and let $z_{i,q}(t)$ be the i th row of $\mathbf{z}_{(q)}(t)$, $\forall i = 1, 2, 3, 4$. With δ_T denoting a constant time-delay, when $q \geq 2$, perform the following computation:

1) For any $\delta_T \neq 0$,

$$\mathbf{z}_{(q-1)}(t) \stackrel{\text{def}}{=} \sum_{i=1}^4 \mathbf{z}_{(q)}(t) z_{i,q}^*(t + \delta_T), \quad (6)$$

where $*$ denotes the complex conjugation.

2) Repeat step 1) for $q = q - 1$ until $\mathbf{z}_{(1)}(t)$ is reached.

For a q -order PPS, in total there are $(q - 1)$ times recursive computation for step 1). When $q = 1$, the frequency of the PPS is a constant, and the PPS is thus a pure-tone. In this case, the proposed algorithm will degenerate to the “univector hydrophone ESPRIT” algorithm in [8], and no recursive computation of steps 1) is required. In addition, it can be used in the multiple-source scenario directly. For details, please refer to [8].

It is known that for every recursive computation of step 1), one-order difference-function of the signal’s phase is derived. Since the phase of the q -order PPS is a q -order polynomial of t , the $(q - 1)$ -order difference-function is a 1-order polynomial. Thus, $\mathbf{z}_{(1)}(t)$ is the 1-order polynomial of t . With some manipulation:

$$\begin{aligned} \mathbf{z}_{(1)}(t) &= \mathbf{a} \left(|\mathbf{a}|_i |^{(2^{(q-2)}-1)} [\mathbf{a}]_i^* \right) \\ &\quad \times e^{j(-1)^{(q-1)} [f(\delta_T, b_{q-1}, b_q) + (q!) b_q \delta_T^{(q-1)} t]} \\ &= \underbrace{\mathbf{a} \left(|\mathbf{a}|_i |^{(2^{(q-2)}-1)} [\mathbf{a}]_i^* \right)}_{\stackrel{\text{def}}{=} \tilde{\mathbf{a}}} \cdot e^{j(-1)^{(q-1)} f(\delta_T, b_{q-1}, b_q)} \\ &\quad \times e^{j(-1)^{(q-1)} (q!) b_q \delta_T^{(q-1)} t}, \quad \forall q \geq 2; \end{aligned} \quad (7)$$

where $[\mathbf{a}]_i$ denotes the i th element in \mathbf{a} , $|\mathbf{a}|_i$ is the absolute value of $[\mathbf{a}]_i$, $q! = 1 \times 2 \times 3 \times \dots \times q$ refers to the factorial of q , and $f(\delta_T, b_{q-1}, b_q)$ is a function of the parameters in the (\cdot) . Note that $f(\delta_T, b_{q-1}, b_q)$ is *independent* of t , and for different q , it has different values.

Equation (7) holds in the single-source scenario and also for the algorithm derived in this section. In the multiple-source scenario, the algorithm to separate the source-of-interest should first be used and the proposed algorithm can then be adopted in a single-source scenario. In the *noisy* case, *multiplicative noise* will be introduced in (6). Equation (7) will become approximated. When the noise power σ^2 increases, the noise will affect the algorithm adversely. With the fixed PPS at the deterministic DOA, when the degree of the PPS increases, the repetitions of step 1) will increase. Thus more *multiplicative noise* will be introduced, which will affect the algorithm more seriously.

Introducing another constant time-delay Δ_T :

$$\begin{aligned} \mathbf{z}_{(1)}(t) &= \tilde{\mathbf{a}} e^{j(-1)^{(q-1)} (q!) b_q \delta_T^{(q-1)} t}, \\ \mathbf{z}_{(1)}(t + \Delta_T) &= \tilde{\mathbf{a}} e^{j(-1)^{(q-1)} (q!) b_q \delta_T^{(q-1)} (t + \Delta_T)} \\ &= \mathbf{z}_{(1)}(t) e^{j(-1)^{(q-1)} (q!) b_q \delta_T^{(q-1)} \Delta_T}. \end{aligned} \quad (8)$$

In practical applications, Δ_T can be the same as or different from δ_T .

The entire 8×1 data set is:

$$\begin{aligned} \mathbf{y} &\stackrel{\text{def}}{=} \begin{bmatrix} \mathbf{z}_{(1)}(t) \\ \mathbf{z}_{(1)}(t + \Delta_T) \end{bmatrix} \stackrel{\text{def}}{=} \begin{bmatrix} \mathbf{y}_1 \\ \mathbf{y}_2 \end{bmatrix} \\ &= \begin{bmatrix} \mathbf{y}_1 \\ \mathbf{y}_1 e^{j(-1)^{(q-1)} b_q (q!) \delta_T^{(q-1)} \Delta_T} \end{bmatrix}. \end{aligned} \quad (10)$$

Note that $e^{j(-1)^{(q-1)} b_q (q!) \delta_T^{(q-1)} \Delta_T}$ depends on (i) the highest-order polynomial-coefficient b_q , (ii) the degree of the polynomial-phase signal q , and (iii) the time-delays $\{\delta_T, \Delta_T\}$, all of which are *constants*. Thus, $e^{j(-1)^{(q-1)} b_q (q!) \delta_T^{(q-1)} \Delta_T}$ is *time-independent* and will be used as the *invariant-factor* in the following ESPRIT [24] algorithm.

Supposing there are N snapshots collected in $\{\mathbf{z}_{(1)}(t), \mathbf{z}_{(1)}(t + \Delta_T)\}$. Then construct the $8 \times N$ data set:

$$\mathbf{Y} \stackrel{\text{def}}{=} [\mathbf{y}(t_1), \mathbf{y}(t_2), \dots, \mathbf{y}(t_N)] = \begin{bmatrix} \mathbf{Y}_1 \\ \mathbf{Y}_2 \end{bmatrix}. \quad (11)$$

The data set \mathbf{Y} in (11) can be seen as a data vector based on the vector $\tilde{\mathbf{a}}$ defined in equation (7) (which is modified from the array-manifold \mathbf{a}). Compute the correlation matrix of the $8 \times N$ data measurements:

$$\mathbf{Y} \mathbf{Y}^H = \begin{bmatrix} \mathbf{Y}_1 \\ \mathbf{Y}_2 \end{bmatrix} [\mathbf{Y}_1^H \mathbf{Y}_2^H] = \begin{bmatrix} \mathbf{Y}_1 \mathbf{Y}_1^H & \mathbf{Y}_1 \mathbf{Y}_2^H \\ \mathbf{Y}_2 \mathbf{Y}_1^H & \mathbf{Y}_2 \mathbf{Y}_2^H \end{bmatrix},$$

and then carry on the eigen-decomposition, where H denotes conjugate transposition.

Similar to Section III-B in [8], there are two estimates of the steering vector $\hat{\mathbf{v}}_1$ (corresponding to $\mathbf{Y}_1 \mathbf{Y}_1^H$), $\hat{\mathbf{v}}_2$ (corresponding to $\mathbf{Y}_2 \mathbf{Y}_2^H$). Since in the present work, we only consider the one-source scenario, these two estimates are obtained from the eigenvector of $\mathbf{Y} \mathbf{Y}^H$ associated with the largest eigenvalue ($\hat{\mathbf{v}}_1$ corresponds to the top 4×1 sub-vector, and $\hat{\mathbf{v}}_2$ corresponds to the bottom 4×1 sub-vector). They are inter-related by the value $\rho = e^{j(-1)^{(q-1)} (q!) b_q \delta_T^{(q-1)} \Delta_T}$, and this ρ can be estimated by the two estimated steering vectors $\hat{\mathbf{v}}_1, \hat{\mathbf{v}}_2$ through: $\hat{\rho} = (\hat{\mathbf{v}}_1^H \hat{\mathbf{v}}_2)^{-1} \hat{\mathbf{v}}_1^H \hat{\mathbf{v}}_2$. The q th-order polynomial coefficient can be estimated by $\hat{b}_q = \frac{\angle \hat{\rho} + 2\pi m_b}{(-1)^{(q-1)} (q!) \delta_T^{(q-1)} \Delta_T}$, where m_b is an integer and can be determined from a prior knowledge of the region of b_q . After the estimation of DOA, the other polynomial coefficients can be estimated from the algorithms derived in the corresponding references. Therefore, $\tilde{\mathbf{a}}$ can be estimated

from $\hat{\mathbf{v}}_1, \hat{\mathbf{v}}_2$ by (within an unknown complex number c): $\hat{\mathbf{a}} = \frac{1}{2} \left(\hat{\mathbf{v}}_1 + \frac{\hat{\mathbf{v}}_2}{\hat{\rho}} \right) = c\tilde{\mathbf{a}}$.

It is worth noting that the algorithm can be used for an *arbitrary* degree polynomial-phase signal (i.e, if $q = 2$, it is an LFM signal). Given the degree of the polynomial-phase signal, the algorithm requires *no* a prior knowledge of the polynomial coefficients. Since the derivation of the matrix-pencil pair depends solely on the degree of the PPS, the efficacy of the proposed algorithm is *independent* of the polynomial coefficients of the signal.

It follows that: $\hat{\mathbf{u}}_x = \frac{[\hat{\mathbf{a}}]_1}{[\hat{\mathbf{a}}]_4}$, $\hat{\mathbf{u}}_y = \frac{[\hat{\mathbf{a}}]_2}{[\hat{\mathbf{a}}]_4}$, $\hat{\mathbf{u}}_z = \frac{[\hat{\mathbf{a}}]_3}{[\hat{\mathbf{a}}]_4}$. Lastly, the direction-of-arrival of the polynomial-phase signal can be estimated by: $\hat{\alpha} = \arccos(\hat{\mathbf{u}}_z)$, $\hat{\beta} = \angle(\hat{\mathbf{u}}_x + j\hat{\mathbf{u}}_y)$, where \angle denotes the angle of the following complex number.

3. SOURCE TRACKING

If the source is moving, the DOA of the source will become time-varying and the array-manifold will change with time. Therefore (1) becomes:

$$\mathbf{a}(\alpha(t), \beta(t)) \stackrel{\text{def}}{=} \begin{bmatrix} \mathbf{u}_x(\alpha(t), \beta(t)) \\ \mathbf{u}_y(\alpha(t), \beta(t)) \\ \mathbf{u}_z(\alpha(t)) \\ 1 \end{bmatrix} = \begin{bmatrix} \sin(\alpha(t)) \cos(\beta(t)) \\ \sin(\alpha(t)) \sin(\beta(t)) \\ \cos(\alpha(t)) \\ 1 \end{bmatrix}.$$

With T_s denoting the sampling time interval, consider there are M time samples. The collected $4 \times M$ data set will be:

$$\mathbf{Z} = [\mathbf{z}(T_s), \mathbf{z}(2T_s), \dots, \mathbf{z}(MT_s)], \quad (12)$$

where $\mathbf{z}(mT_s) = \mathbf{a}(\alpha(mT_s), \beta(mT_s))s(mT_s) + \mathbf{n}(mT_s)$, $\forall m = 1, 2, \dots, M$.

Consider the first $(q+1)$ data vectors in (12), $[\mathbf{z}(T_s), \mathbf{z}(2T_s), \dots, \mathbf{z}((q+1)T_s)]$. Recall the pre-processing steps of the data-sets in Section 2 by setting $\delta_T = T_s$, and presume the elevation-azimuth angle of the source remains the same during the time interval $(q+1)T_s$. For a q -order polynomial-phase signal, perform one more computation of step 1) from the above $(q+1)$ data vectors, and in total, there will be q times computation. The following result will be obtained:

$$\check{\mathbf{z}}(T_s) = \check{\mathbf{a}}(\alpha(T_s), \beta(T_s))e^{j(-1)^q b_q(q!)T_s^q}, \quad (13)$$

$$\check{\mathbf{a}} \stackrel{\text{def}}{=} \mathbf{a} \left(\left| [\mathbf{a}]_i \right|^{(2^{(q-1)})} [\mathbf{a}]_i^* \right). \quad (14)$$

Similarly, from any $(q+1)$ contiguous data vectors in (12), $[\mathbf{z}(nT_s), \mathbf{z}((n+1)T_s), \dots, \mathbf{z}((n+q)T_s)]$, we can obtain: $\check{\mathbf{z}}(nT_s) = \check{\mathbf{a}}(\alpha(nT_s), \beta(nT_s))e^{j(-1)^q b_q(q!)T_s^q}$, $\forall n = 1, (M-q)$. The following problem is to adaptively estimate $(\alpha(nT_s), \beta(nT_s))$ over $n = 1, 2, \dots, (M-q)$, from $[\check{\mathbf{z}}(T_s), \check{\mathbf{z}}(2T_s), \dots, \check{\mathbf{z}}((M-q)T_s)]$. The algorithms in [1, 25, 26] can be adopted for the source-tracking of the polynomial-phase signal. The above manipulations extract the relation among the $(q+1)$ adjacent data sets for the polynomial-phase signal. The estimate based

on $[\check{\mathbf{z}}(T_s), \check{\mathbf{z}}(2T_s), \dots, \check{\mathbf{z}}((M-q)T_s)]$ will thus outperform the estimate from $[\mathbf{z}(T_s), \mathbf{z}(2T_s), \dots, \mathbf{z}(MT_s)]$ directly. The simulation results in Section 4 verify this point. The following reviews the “single-forgetting-factor tracking” algorithm in [25, 26].

The recursive least-squares algorithm is used for the source-tracking in [25, 26] as:

$$\hat{\mathbf{a}}(nT_s) = \frac{\Re\{\check{\mathbf{z}}(nT_s)\}}{\Re\{[\check{\mathbf{z}}(nT_s)]_4\}},$$

$$\hat{\mathbf{a}}_N = [\hat{\mathbf{u}}_{x,N}, \hat{\mathbf{u}}_{y,N}, \hat{\mathbf{u}}_{z,N}, 1]^T = \frac{\sum_{n=0}^N \lambda^{-n} \hat{\mathbf{a}}(nT_s)}{\sum_{n=0}^N \lambda^{-n}},$$

where $\lambda < 1$ denotes a “forgetting factor” and $\Re\{\cdot\}$ denotes the real-value part of the entity inside $\{\cdot\}$. It follows that the recursive relation is obtained:

$$\hat{\mathbf{a}}(nT_s) = \lambda \hat{\mathbf{a}}(nT_s - T_s) + (1-\lambda) \hat{\mathbf{a}}(nT_s), \quad \forall n = 1, 2, \dots, N.$$

Hence, $\hat{\alpha}_N = \arccos(\hat{\mathbf{u}}_{z,N})$, $\hat{\beta}_N = \angle(\hat{\mathbf{u}}_{x,N} + j\hat{\mathbf{u}}_{y,N})$. For the Multiple-Forgetting-Factor (MFF) tracking approach in [25, 26], the described pre-processing technique can also be adopted.

4. MONTE CARLO SIMULATION

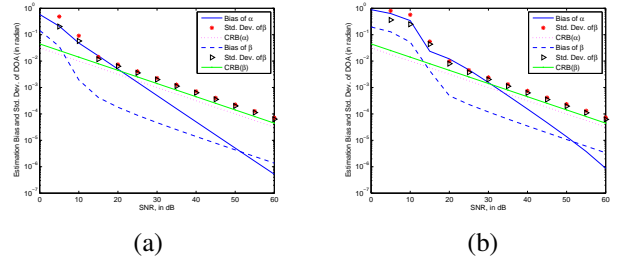


Fig. 1: Estimation bias and standard deviations of $\{\alpha, \beta\}$ with (a) 2-order, and (b) 4-order PPS versus SNR.

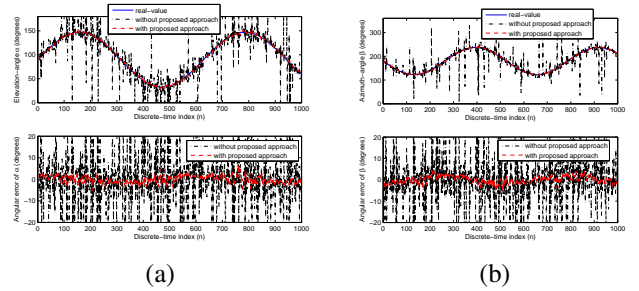


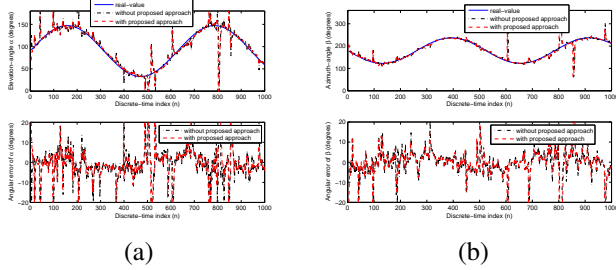
Fig. 2: Single-forgetting-factor tracking ($\lambda = 0.7$) and angular error of the (a) elevation-angle, and (b) azimuth-angle for a PPS source. ‘without proposed approach’ means using the method in [26] directly, and ‘with proposed approach’ denotes incorporating the proposed pre-processing technique in Section 3.

4.1. Examples for Direction Finding

A 2-order unity power polynomial-phase signal (a.k.a. LFM or Chirp signal) with $\{b_0 = 0.05, b_0 = 0.1, b_2 = 0.13\}$ is

Table 1: Angular Error and Standard Deviations of Source Tracking (in degree)

	$\lambda_1 (\lambda)$	λ_2	λ_3	Mean of α_r	Std. Dev. of α_r	Mean of β_r	Std. Dev. of β_r
MFF without the proposed technique	0.9	0.8	0.7	-1.021	11.47	0.459	16.09
MFF with the proposed technique	0.9	0.8	0.7	-0.975	11.18	0.700	15.36
SFF without the proposed technique	0.9	—	—	-0.478	21.55	-1.561	23.18
SFF with the proposed technique	0.9	—	—	-0.233	3.742	0.200	4.065
SFF without the proposed technique	0.8	—	—	-0.376	24.45	-0.433	28.00
SFF with the proposed technique	0.8	—	—	-0.134	1.853	0.071	1.930
SFF without the proposed technique	0.7	—	—	0.497	20.89	-0.123	28.17
SFF with the proposed technique	0.7	—	—	-0.089	1.689	0.187	1.570

**Fig. 3:** Multiple-forgetting-factor tracking ($\lambda_1 = 0.9, \lambda_2 = 0.8, \lambda_3 = 0.7$) and angular error of the (a) elevation-angle, and (b) azimuth angle for a PPS source.

used in this example. The direction-of-arrival of the source is $\{\alpha, \beta\} = \{45^\circ, 60^\circ\}$. Figure 1(a) plots the estimation bias and standard deviations of DOA $\{\alpha, \beta\}$ versus signal-to-noise ratio (SNR) ($1/\sigma^2$). 1000 trials are used for each data point on each graph and these estimates use 500 temporal snapshots. When $\text{SNR} \geq 15\text{dB}$, the standard deviations are very close to Cramér-Rao lower bounds. When the SNR is low ($\text{SNR} \leq 10\text{dB}$), the noise affects the algorithm seriously. Thus there is a visible gap between the standard deviations and the Cramér-Rao bounds. This is because the *multiplicative* noise is introduced when equation (6) is used to derive the data set \mathbf{Y} . But when $\text{SNR} \geq 15\text{dB}$, the noise effect decreases, hence the estimation standard deviations decrease in parallel with the Cramér-Rao bounds when the SNR increases. Figure 1(b) plots the estimation bias and standard deviations of $\{\alpha, \beta\}$ in a 4-order polynomial-phase signal scenario with $\{b_0 = 0.05, b_1 = 0.1, b_2 = 0.13, b_3 = 0.23, b_4 = 0.29\}$.

4.2. Examples for Source Tracking

The time-varying elevation-azimuth angle of the 2-order moving polynomial-phase signal is modeled as: $\alpha(nT_s) = \alpha_0 + \sin(\omega_\alpha nT_s), \beta(nT_s) = \beta_0 + \sin(\omega_\beta nT_s)$, with $(\alpha_0, \beta_0) = (90^\circ, 180^\circ), (\omega_\alpha, \omega_\beta) = (0.01, -0.012)$, and $n = 1, \dots, 1000$. Figure 2 plots the loci of the source's elevation-angle and azimuth-angle with the single-forgetting-factor (SFF) tracking algorithm ($\lambda = 0.7$), at $\text{SNR} = 20\text{dB}$. The angular errors of $\{\alpha, \beta\}$ are also plotted. Figure 3 plots the loci of the source's elevation-azimuth angle and the angular errors with the multiple-forgetting-factor (MFF) tracking algorithm ($\lambda_1 = 0.9, \lambda_2 = 0.8, \lambda_3 = 0.7$). Both the results with and without the proposed pre-processing technique are presented in these figures. Table 1 summarizes the angular errors and standard deviations of elevation-angle α_r and azimuth-angle

β_r for source tracking with different methods. Qualitative observations obtained from Table 1 are listed below: 1) Both the performances of SFF and MFF methods incorporating the proposed technique in Section 3 are better than their counterparts without incorporating the proposed technique. This can be seen from the standard deviations of (α_r, β_r) . 2) The performance of SFF method incorporating the proposed technique improves significantly in a wide region of λ compared with its counterpart without incorporating the proposed technique. The result is even better than the MFF method, both with and without the proposed technique. 3) For the SFF algorithm incorporating the proposed technique, the standard deviations of (α_r, β_r) decline when λ increases. 4) The performance of MFF method without the proposed technique is better than the performance of SFF method without the proposed technique. This is expected and consistent with the results reported in [26].

It can be seen that with the proposed technique, the source tracking performance can improve significantly with less computation workload because the performance of the SFF approach surpasses those of the other methods. For the comparison of the computation workload between the SFF and the MFF methods, please refer to [25].

5. CONCLUSION

An ESPRIT-based algorithm for azimuth-elevation direction-finding of one broadband polynomial-phase signal with an arbitrary degree is investigated in this paper using a single acoustic vector sensor. This is the first time in the literature to use an acoustic vector sensor to estimate the direction-of-arrival of a polynomial-phase signal with an arbitrary degree. The adaptive tracking algorithms of both the single-forgetting-factor approach and the multiple-forgetting-factor approach are also adapted to incorporate the proposed pre-processing technique to track a polynomial-phase signal utilizing one acoustic vector sensor. From the simulation results, the single-forgetting-factor approach with the proposed pre-processing technique can provide better performance than its counterpart without pre-processing technique, and can even offer better performance than the multiple-forgetting-factor approach. An electromagnetic counterpart of the algorithm exists in [18, 27]. However, the proposed algorithmic steps are fundamentally different from [18, 27] due to the fundamental differences between acoustics and electromagnetics.

6. REFERENCES

- [1] A. Nehorai and E. Paldi, "Acoustic vector-sensor array processing," *IEEE Transactions on Signal Processing*, vol. 42, no. 2, pp. 2481–2491, September 1994.
- [2] K. T. Wong and M. D. Zoltowski, "Closed-form underwater acoustic direction-finding with arbitrarily spaced vector-hydrophones at unknown locations," *IEEE Journal of Oceanic Engineering*, vol. 22, no. 3, pp. 566–575, July 1997.
- [3] K. T. Wong and M. D. Zoltowski, "Extended-aperture underwater acoustic multisource azimuth/elevation direction-finding using uniformly but sparsely spaced vector hydrophones," *IEEE Journal of Oceanic Engineering*, vol. 22, no. 4, pp. 659–672, October 1997.
- [4] M. Hawkes and A. Nehorai, "Acoustic vector-sensor beamforming and capon direction estimation," *IEEE Transactions on Signal Processing*, vol. 46, no. 9, pp. 2291–2304, September 1998.
- [5] K. T. Wong and M. D. Zoltowski, "Root-music-based azimuth-elevation angle-of-arrival estimation with uniformly spaced but arbitrarily oriented velocity hydrophones," *IEEE Transactions on Signal Processing*, vol. 47, no. 12, pp. 3250–3260, December 1999.
- [6] K. T. Wong and M. D. Zoltowski, "Self-initiating music-based direction finding in underwater acoustic particle velocity-field beamspace," *IEEE Journal of Oceanic Engineering*, vol. 25, no. 2, pp. 262–273, April 2000.
- [7] M. D. Zoltowski and K. T. Wong, "Closed-form eigenstructure-based direction finding using arbitrary but identical subarrays on a sparse uniform cartesian array grid," *IEEE Transactions on Signal Processing*, vol. 48, no. 8, pp. 2205–2210, August 2000.
- [8] P. Tichavský, K. T. Wong, and M. D. Zoltowski, "Near-field/far-field azimuth and elevation angle estimation using a single vector hydrophone," *IEEE Transactions on Signal Processing*, vol. 49, no. 11, pp. 2498–2510, November 2001.
- [9] K. T. Wong, Y. I. Wu, and S.-K. Lau, "The acoustic vector-sensor's near-field array-manifold," *IEEE Transactions on Signal Processing*, vol. 58, no. 7, pp. 3946–3951, July 2010.
- [10] X. Yuan, "Coherent source direction-finding using a sparsely-distributed acoustic vector-sensor array," *IEEE Transactions on Aerospace and Electronic Systems*, vol. 48, no. 3, pp. 2710–2715, July 2012.
- [11] X. Yuan, "Direction-finding with a misoriented acoustic vector sensor," *IEEE Transactions on Aerospace and Electronic Systems*, vol. 48, no. 2, pp. 1809–1815, April 2012.
- [12] X. Yuan, "Cramer-rao bounds of direction-of-arrival and distance estimation of a near-field incident source for an acoustic vector-sensor: Gaussian source and polynomial-phase source," *IET Radar, Sonar and Navigation*, vol. 6, no. 7, pp. 638–648, July 2012.
- [13] Y. Song and K. T. Wong, "Lower bound of direction-of-arrival estimation for acoustic vector sensor with sensor breakdown," *IEEE Transactions on Aerospace and Electronic Systems*, vol. 48, no. 4, pp. 3703–3708, October 2012.
- [14] Y. Song and K. T. Wong, "Azimuth-elevation direction finding, using a microphone and three orthogonal velocity-sensors as a noncollocated subarray," *Journal of the Acoustical Society of America*, vol. 133, no. 4, pp. 1987–1995, April 2013.
- [15] M. Adjrad and A. Belouchrani, "Estimation of multicomponent polynomial-phase signals impinging on a multisensor array using state-space modeling," *IEEE Transactions on Signal Processing*, vol. 55, no. 1, pp. 32–45, January 2007.
- [16] G. M. Phillips, *Interpolation and Approximation by Polynomials*, New York, U.S.A.: Springer, 2003.
- [17] X. Yuan, "Direction-finding wideband linear fm sources with triangular arrays," *IEEE Transactions on Aerospace and Electronic Systems*, vol. 48, no. 3, pp. 2416–2425, July 2012.
- [18] X. Yuan, "Estimating the DOA and the polarization of a polynomial-phase signal using a single polarized vector-sensor," *IEEE Transactions on Signal Processing*, vol. 60, no. 3, pp. 1270–1282, March 2012.
- [19] P. Wang, I. Djurovic, and J. Yang, "Generalized high-order phase function for parameter estimation of polynomial phase signal," *IEEE Transactions on Signal Processing*, vol. 56, no. 7, pp. 3023–3028, July 2008.
- [20] P. Wang, H. Li, I. Djurovic, and B. Himed, "Instantaneous frequency rate estimation for high-order polynomial-phase signals," *IEEE Signal Processing Letters*, vol. 16, no. 9, pp. 782–785, September 2009.
- [21] N. Ma and J. T. Goh, "Ambiguity-function-based techniques to estimate doa of broadband chirp signals," *IEEE Transactions on Signal Processing*, vol. 54, no. 5, pp. 1826–1839, May 2006.
- [22] A. Amar, "Efficient estimation of a narrow-band polynomial phase signal impinging on a sensor array," *IEEE Transactions on Signal Processing*, vol. 58, no. 2, pp. 923–927, February 2010.
- [23] A. Leshem, A. Amar, and A. van der Veen, "A low complexity blind estimator of narrowband polynomial phase signals," *IEEE Transactions on Signal Processing*, vol. 58, no. 9, pp. 4674–4683, September 2010.
- [24] R. Roy and T. Kailath, "ESPRIT - estimation of signal parameters via rotational invariance techniques," *IEEE Transactions on Acoustics, Speech, and Signal Processing*, vol. 37, no. 7, pp. 984–995, July 1989.
- [25] A. Nehorai and P. Tichavský, "Cross-product algorithms for source tracking using an em vector sensor," *IEEE Transactions on Signal Processing*, vol. 47, no. 10, pp. 2863–2867, October 1999.
- [26] M. K. Awad and K. T. Wong, "Recursive least-squares source-tracking using one acoustic vector-sensor," *IEEE Transactions on Aerospace and Electronic Systems*, vol. 48, no. 4, pp. 3073–3083, October 2012.
- [27] X. Yuan, "Polynomial-phase signal source-tracking using an electromagnetic vector-sensor," *International Conference on Acoustics, Speech, and Signal Processing (ICASSP)*, pp. 2577–2580, March 2012.